Localization of Cell Surface Sites Involved in Fibronectin Fibrillogenesis

Donna M. Pesciotta Peters and Deane F. Mosher

Departments of Medicine and Physiological Chemistry, University of Wisconsin, Madison, Wisconsin 53706

Abstract. Fibronectin binding sites on cultured human fibroblasts were localized by high voltage electron microscopy using either 5- or 18-nm colloidal gold beads (Au_5 or Au_{18}) bound to intact fibronectin, the 70-kD amino-terminal fragment of fibronectin that blocks incorporation of exogenous fibronectin into extracellular matrix, or 160–180-kD fragments of fibronectin with cell adhesion and heparin-binding activities. Binding sites for Au_{18}-fibronectin on the cell surface were localized to specific regions along the edge of the fibroblast and on retraction fibers. Au_{18}-fibronectin complexes at these sites were initially localized in clusters that co-aligned with intracellular microfilament bundles. With longer incubations, Au_{18}-fibronectin complexes were arranged into long fibrillar networks on the cell surface and in the extracellular space. The appearance of Au_{18}-fibronectin in these fibrillar networks and disappearance of clusters of Au_{18}-fibronectin suggest that Au_{18}-fibronectin complexes are arranged into matrix at specific regions of the cell surface. Au_{18}-70-kD fragment complexes initially had a similar distribution to Au_{18}-fibronectin complexes. With longer incubations, Au_{18}-70-kD fragment complexes were found in long linear arrangements on the cell surface. Double labeling experiments using Au_{18}-70-kD fragment and Au_5-160–180-kD fragments showed that the 70-kD fragment and the 160–180-kD fragments bind to different regions of the cell.

FIBRONECTIN is a connective tissue glycoprotein that consists of two structurally similar but not necessarily identical disulfide-bonded subunits (Schwarzbauer et al., 1985; Sekiguchi et al., 1985). There are two principle types of fibronectin: (*a*) plasma fibronectin, which appears to be produced by hepatocytes (Tamkun and Hynes, 1983) and is found in the circulation, and (*b*) cellular fibronectin, which is synthesized by a variety of cell types (for recent reviews see Mosher, 1984; Hynes, 1985). Both types of fibronectin are structurally similar, except for an additional type III homology sequence found in cellular fibronectin (Kornblihtt et al., 1984).

Both types of fibronectin can be found in a soluble form in blood, other body fluids, and culture medium, and in an insoluble, usually fibrillar, form in the extracellular space of connective tissues, basement membranes, and cultured cells. Fibronectin found in fibrils can come from either exogenously added plasma fibronectin or cellular fibronectin (Hayman and Ruoslahti, 1979; Oh et al., 1981).

It is not clearly understood how fibronectin and other macromolecules of the extracellular matrix are assembled into an extracellular matrix. In cultured fibroblasts and embryonic tendon and corneal fibroblasts it has been shown that fibronectin (Hedman et al., 1978) and collagen (Trelstad and Hayashi, 1979) fibril formation occur in close association with the fibroblast cell surface. These observations suggest that cells may play a role in regulation of the formation of the extracellular matrix. One way cells can influence the formation of the extracellular matrix is by control of the stoichiometry and sequential appearance of secreted extracellular matrix components. Another way is by events mediated at the cell surface. Recently, a presumptive cell surface receptor that mediates the fibrillogenesis of exogenous fibronectin into extracellular matrix fibrils has been described (McKeown-Longo and Mosher, 1983; 1985). The receptor appears to interact primarily with the 70-kD amino-terminal gelatin- and heparin-binding region of fibronectin, rather than with the site on fibronectin that mediates cell adhesion (McKeown-Longo and Mosher, 1985).

In the present study, we have used high voltage electron microscopy (HVEM)[1] to identify sites in the cell layer where exogenous fibronectin and fragments of fibronectin bind, and to study the relationship between cellular structures and extracellular matrix fibrils during fibrillogenesis. For this, human skin fibroblasts in culture were incubated with 18-nm gold beads (Au_{18}) coupled to either fibronectin or the 70-kD fragment of fibronectin that contains the type I and II homology units important for binding to the presumptive matrix assembly receptor. Fragments of fibronectin containing the majority of the type III homology units and such cell binding domains as the cell adhesion and heparin-binding sites (Pierschbacher et al., 1981; McKeown-Longo and Mosher, 1985) were bound to 5-nm colloidal gold beads (Au_5), and were used to distinguish other binding sites on fibronectin (Pytela et al., 1985; Akiyama et al., 1986) from the presumptive matrix assembly receptor binding sites.

1. *Abbreviations used in this paper*: Au_5, 5-nm colloidal gold beads; Au_{18}, 18-nm colloidal gold beads; HVEM, high voltage electron microscopy.

Materials and Methods

Cell Culture and Labeling Conditions

Embryonic human skin S132 fibroblasts (obtained from Dr. Michael Gould, University of Wisconsin) and Detroit 551 fibroblasts (American Type Culture Collection, Rockville, MD) were grown in Ham's F-12 media supplemented with 10% fetal calf serum and in minimum essential media supplemented with 1 mM sodium pyruvate and 10% fetal calf serum, respectively. Neonatal human foreskin A1-F fibroblasts (obtained from Dr. Lynn Allen-Hoffmann, University of Wisconsin) were grown in Ham's F-12 media supplemented with 15% fetal calf serum.

Fibroblasts were seeded and incubated for 3–4 d in the appropriate media on sterile Formvar-coated gold grids on glass coverslips (Wolosewick and Porter, 1976). The fibroblasts were washed three times with Hank's balanced salt solution and placed in fresh media containing 0.2% bovine albumin and Au_{18}-fibronectin (7.0 μg/ml), Au_{18}-70-kD fragment (13 μg/ml), Au_5-cell adhesion fragments (90 μg/ml), or Au_{18}-bovine albumin (1.5 mg/ml). The fibroblasts were incubated for 0.25, 0.5, 1.5, 3, or 5 h at 37°C.

Preparation of Colloidal Gold Fibronectin or Fibronectin Fragments

Colloidal gold beads 18 nm in diameter (Au_{18}) were prepared by adding 0.5 ml of 4% gold chloride to 200 ml deionized distilled water (Geoghegan and Ackerman, 1977). To this, 5 ml of freshly prepared 1% tri-sodium citrate was added, and the mixture was boiled under reflux for 30 min until the color turned from brown to red. The colloidal gold sol was filtered through a 0.45-μm millipore filter and stored at 4°C. Colloidal gold beads 5 nm in diameter (Au_5) that had been prepared using white phosphorus were kindly provided by Dr. Ralph Albrecht, University of Wisconsin.

Colloidal gold beads were added to fibronectin, fibronectin fragments, or bovine albumin using a modification of the Geoghegan and Ackerman (1977) procedure. Colloidal gold sol (Au_{18}) was adjusted to pH 7.0 with 0.2 N potassium carbonate and filtered through a 0.45-μm millipore filter. The minimum concentration of fibronectin needed to stabilize 1 ml of the gold sol was determined with an adsorption isotherm (Horisberger and Rosset, 1977) and found to be between 5 and 10 μg of plasma fibronectin in 2 mM Tris-HCl, 15 mM sodium chloride, pH 7.4. This minimum concentration of plasma fibronectin plus an extra 20% was slowly added to the adjusted gold sol and incubated for 5 min at 23°C. Unbound areas on the gold beads were blocked with 1% polyethylene glycol (final concentration 0.05%) filtered through a 0.2-μm filter. Au_{18}-fibronectin was centrifuged at 28,000 *g* for 30 min at 4°C. The protein-gold complex was resuspended into sterile 0.1 M Hepes, pH 7.0 (final $OD_{520\ nm}$ ~3.6) and stored at 4°C. The biological activity of gold-fibronectin complex was assayed in cell-binding assays (McKeown-Longo and Mosher, 1983) comparing ^{125}I-fibronectin and ^{125}I-fibronectin bound to gold. The ^{125}I-fibronectin-gold complex retained ~60% of the cell-binding activity of uncomplexed ^{125}I-fibronectin. Colloidal gold complexed to fibronectin fragments were prepared in a similar manner except that the pH of the colloidal gold sol was 7.2. Albumin in water (10% wt/vol) was bound to colloidal gold sol at pH 9.0.

Preparation of Fibronectin and Fibronectin Fragments

Plasma fibronectin was purified from a commercial by-product of human plasma Factor VIII production (Mosher and Johnson, 1983).

The 70-kD fragment of fibronectin (Balian et al., 1979) was prepared by digesting fibronectin (2 mg/ml) with cathepsin D (3 μg/ml) in 50 mM sodium acetate buffer, pH 3.5, containing soybean trypsin inhibitor (3.2 μg/ml), and phenylmethylsulfonyl fluoride (8 μg/ml) for 16 h at 37°C. The digestion was initiated by forcefully injecting a concentrated fibronectin solution (which was in 10 mM Tris-HCl, 0.15 M sodium chloride, pH 7.4) underneath the surface of the acetate buffer containing the cathepsin D, taking care to avoid foaming. The digestion was stopped with pepstatin A (0.2 μg/ml) and titration to pH 7.4 with 0.5 M Tris base. The digest was then placed on a gelatin–sepharose column equilibrated with 20 mM Tris-HCl, 0.15 M sodium chloride, pH 7.4, and the gelatin-binding 70- and 40-kD fragments of fibronectin were eluted with 3 M guanidine-HCl in 20 mM Tris-HCl, 0.15 M sodium chloride, pH 7.4. The 70-kD fragment was purified free of the contaminating 40-kD fragment on a Sephadex G-100 column (94 × 3.5 cm) equilibrated with 20 mM Tris-HCl, 0.15 M sodium chloride, pH 7.4. Polyacrylamide slab gel electrophoretic analysis in the presence of sodium dodecyl sulfate showed that the purified fragment migrated as a single band with an apparent size of 70 kD (data not shown).

Fragments containing the type III homology units of fibronectin were prepared by digesting reduced and alkylated fibronectin with trypsin (1 μg/ml) for 15 min at 37°C (Williams et al., 1983). Previous sodium dodecyl sulfate polyacrylamide slab gel electrophoretic analysis of the tryptic digest showed that the digest contained two major bands with apparent molecular masses of 160–180 kD (see Fig. 5 in Williams et al., 1983). The 160–180-kD fragments were purified on a Sepharose 6B column as described by McKeown-Longo and Mosher (1985) to remove small contaminating fragments. The 160–180-kD fragments were further purified on a gelatin–sepharose affinity column (Engvall and Ruoslahti, 1977) to remove any fragments that retained an intact gelatin-binding region. The purified 160–180-kD fragments were found to promote cell adhesion and spreading of human skin fibroblasts (McKeown-Longo and Mosher, 1985) and to bind to heparin-agarose in the presence of Tris-HCl buffer (pH 7.4), 0.1 M sodium chloride (data not shown). Upon electrophoresis, only bands in the 160–180-kD region were detected (data not shown).

HVEM

Labeled fibroblasts were washed three times with Hank's balanced salt solution and fixed for 30 min with 2.5% glutaraldehyde in 0.1 M Hepes, pH 7.0, containing 0.05% saponin and 0.2% tannic acid (Maupin and Pollard, 1983). Fixed fibroblasts were washed for 1 h (four changes) with 0.1 M Hepes, pH 7.0, and for 5 min (two changes) with distilled water. Cells were stained for 10 min with 1% uranyl acetate in water, dehydrated in a graded series of ethanol (20–100%), and critical point dried with a Samdri PVT3 (Touisimis, Rockville, MD) (Ris, 1985). Critical point dried samples were carbon coated and examined with the AEI.EM7 high voltage electron microscope at the University of Wisconsin, Madison, WI. All labeling experiments were performed three times. Between 25 and 60 different cells were photographed for each set of conditions.

Transmission Electron Microscopy

Fibroblasts were grown for either 3 d or until confluency on glass coverslips and labeled for 30 min with Au_{18}-fibronectin as described above. The cells were washed with Hank's balanced salt solution and fixed with 2.5% glutaraldehyde in 0.1 M Hepes, pH 7.0, containing 0.05% saponin and 0.2% tannic acid (Maupin and Pollard, 1983). Fixed fibroblasts were washed for 1 h with 0.1 M Hepes, pH 7.0, postfixed with 0.1% osmium tetroxide, 0.1 M Hepes, pH 7.0, for 10 min, and washed with distilled water for 10 min (two changes). Cells were stained with 1.0% uranyl acetate in water for 10 min, dehydrated in a graded series of ethanol (20–100%), and infiltrated with a graded series of epon-araldite 812 resin mixture (25–100%). Thin sections were cut with a microtome (Reichert Scientific Instruments, Buffalo, NY), stained for 30 min with 7.5% magnesium acetate, and counterstained with lead citrate for 10 min. Thin sections were examined with a Jeol 100C electron microscope.

Analysis of High Voltage Electron Micrographs

Micrographs from three different experiments on subconfluent cells were randomly chosen for analysis. Individual cells were scored as to whether they had no label, label only in clusters, label both in clusters and fibril-like arrangements, or label only in fibril-like arrangements. Surface areas with the various labeling patterns were determined using an IBM-XT computer equipped with a Micro-plan II image analysis systems (Lab computer system) and the Symphony program by Lotus.

Results

Localization of Au_{18}-Fibronectin Complexes to the Fibroblast Cell Surface

To learn if exogenous fibronectin bound to the cell surface and to identify cell surface structures potentially involved in the assembly of fibronectin fibrils, binding of Au_{18}-fibronectin to subconfluent cultures of human skin fibroblasts and assembly of Au_{18}-fibronectin into fibrils were monitored by HVEM.

Fig. 1 is a stereo micrograph of a whole mount from a 4-d-old subconfluent culture of embryonic skin fibroblasts (S132) incubated with Au_{18}-fibronectin for 15 min at 37°C. The

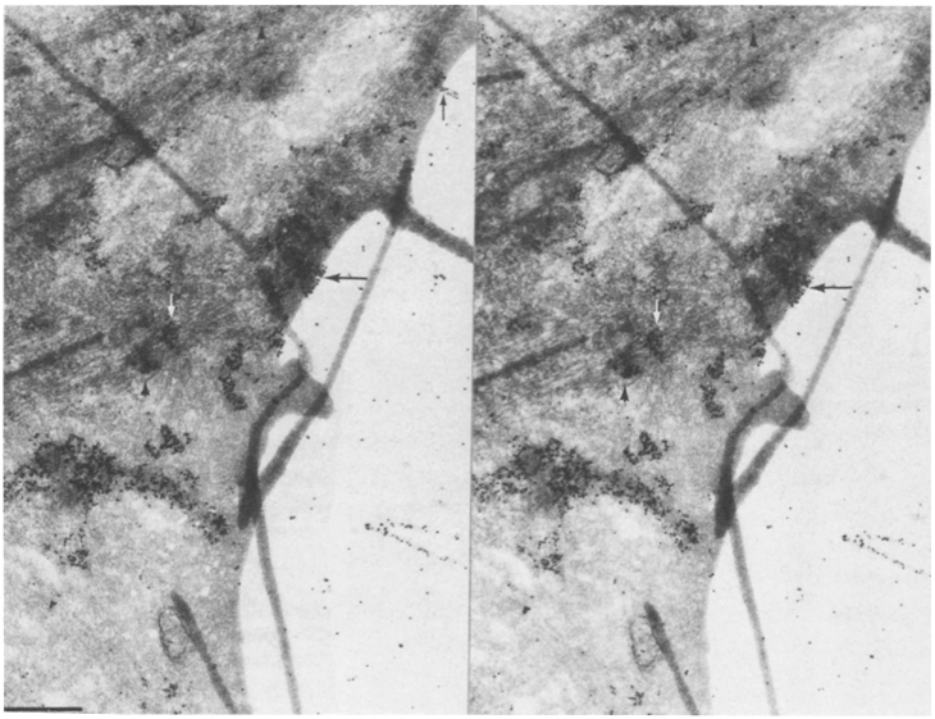

Figure 1. A stereo micrograph of a whole mount of an embryonic human skin fibroblast (S132) incubated with Au_{18}-fibronectin for 15 min at 37°C. Clusters of Au_{18}-fibronectin and single beads of Au_{18}-fibronectin on the dorsal surface of the fibroblast (*arrowheads*) and on the ventral surface of the cell facing the substratum (*white arrow*) appear to co-align with intracellular microfilaments. Au_{18}-fibronectin clusters are also seen wrapping around the edge of the cell (*large arrows*) and on the dorsal surface connected to filaments of Au_{18}-fibronectin (*small arrow*). Stereo tilt 7.4° from horizontal. Bar, 0.5 μm.

micrograph shows labeling patterns that were observed on the three fibroblasts strains studied (S132, Detroit 551, and A1-F). Au_{18}-fibronectin was frequently found in clusters on the upper and lower surfaces of the cell. These clusters were predominantly located along the retracting and lateral edges of the fibroblast. Many of the clusters and single beads of Au_{18}-fibronectin on the top of the cell co-aligned with intracellular bundles of cytoskeleton microfilaments presumed to contain actin (Fig. 1, arrowheads). Clusters of Au_{18}-fibronectin underneath the cell also appear to co-align with intracellular microfilament bundles (white arrow). Along the edge of the cell shown in Fig. 1, a cluster of Au_{18}-fibronectin is seen wrapping around the cell (large arrow). In the upper right hand corner of the micrograph, a small cluster of Au_{18}-fibronectin on top of the cell membrane has two to three small filaments containing Au_{18}-fibronectin coming off the cluster (small arrow). Small filaments containing Au_{18}-fibronectin are also observed on the Formvar surface.

In fibroblast cultures incubated with Au_{18}-fibronectin for 15–30 min, 93% of the fibroblasts observed were labeled with Au_{18}-fibronectin (Table I). Au_{18}-fibronectin was observed bound to fibroblasts in either clusters or fibrillar arrangements. The majority of the fibroblasts (63%) contained Au_{18}-fibronectin arranged in clusters. These clusters were 0.4×10^{-3}–3.0×10^{-1} μm² in area. The average area of a cluster was 0.3×10^{-1} μm², and the clusters covered ~0.18% of the area observed (Table II).

The cell surface labeling pattern of Au_{18}-fibronectin was specific inasmuch as it was not seen when fibroblasts were incubated with a 100-fold excess (700 μg/ml) of unlabeled fibronectin along with Au_{18}-fibronectin. Fig. 2 *A* shows an A1-F skin fibroblast labeled in the presence of excess fibronectin. Au_{18}-fibronectin beads on the cell surface are few and scattered (arrows). The Au_{18}-fibronectin that is present does not appear to co-align with the microfilament bundles. As a further test of specificity, human fibroblasts were also labeled with Au_{18}-albumin for 15 min at 37°C (Fig. 2 *B*). There is no cell surface labeling along microfilament bundles and only a few scattered beads on the cell surface (arrows).

The cell surface labeling pattern was examined in 3-4-d-old cultures of fibroblasts by conventional transmission electron microscopy. Fig. 3 shows a longitudinal section of an A1-F fibroblast incubated with Au_{18}-fibronectin for 30 min. Clusters of Au_{18}-fibronectin are found on the cell surface above microfilament bundles (Fig. 3, *A* and *C*, arrows). The Au_{18}-fibronectin on the cell surface does not appear to be associated with any filamentous cell surface material, but rather appears to be bound directly to the cell membrane. Au_{18}-fibronectin complexes bound to the cell surface could be competitively inhibited with excess unlabeled fibronectin (data not shown). Since growth and labeling conditions for the cells studied by transmission electron microscopy were identical to conditions for the fibroblasts studied in the HVEM as whole mounts, it seems likely that the Au_{18}-fibronectin complexes observed in the whole mounts by HVEM were also directly bound to the cell surface.

Table I. Patterns of Labeling of Human Skin Fibroblasts with Au_{18}-Fibronectin

Labeling conditions	No. of cells	Labeled cells			
		Clusters	Clusters and fibrils	Fibrils	No label
		%	%	%	%
Au_{18}-fibronectin (15–30 min)	27	63	15	15	7
Au_{18}-fibronectin (1.5–5 h)	19	11	63	16	11

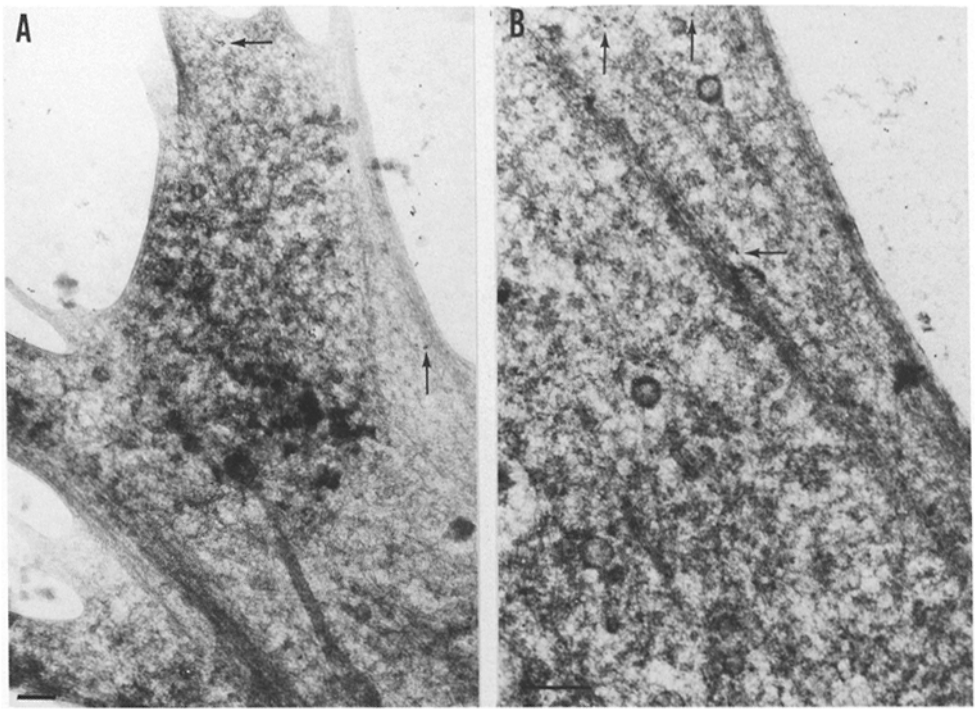

Figure 2. (*A*) A whole mount of an Al-F skin fibroblast incubated with Au_{18}-fibronectin and a 100-fold excess of plasma fibronectin for 30 min at 37°C. Arrows show scattered Au_{18}-fibronectin complexes on the dorsal surface. (*B*) A whole mount of a human skin S132 fibroblast incubated with Au_{18}-albumin complexes for 15 min at 37°C. Arrows show scattered Au_{18}-albumin complexes on the cell surface. Bars, 0.5 μm.

Under transmission electron microscopy, some Au_{18}-fibronectin was found to be associated with filamentous material on the cell surface and in some instances in the extracellular matrix above the fibroblast (Fig. 3, *B* and *C*, small arrows). Au_{18}-fibronectin complexes bound to the extracellular matrix could not be competitively inhibited with excess unlabeled fibronectin (data not shown) and may represent one source of the large nonspecific binding fraction reported earlier (McKeown-Longo and Mosher, 1983). Some endocytosis of the Au_{18}-fibronectin complexes was observed (Fig. 3 *D*), but the amount of Au_{18}-fibronectin taken up by endocytosis represented <1% of the complexes. Au_{18}-fibronectin complexes are seen bound to the substratum in a random distribution (Fig. 3 *E*).

When confluent fibroblast cultures containing numerous extracellular fibrils were labeled with Au_{18}-fibronectin for 30 min and examined by transmission electron microscopy, Au_{18}-fibronectin was observed on the cell surface as well as in matrix fibrils (data not shown). Binding of Au_{18}-fibronectin to cell surfaces of these confluent cultures was specific and could be blocked with unlabeled fibronectin. Matrix bound Au_{18}-fibronectin, on the other hand, could not be competitively inhibited with excess unlabeled fibronectin.

Reorganization of Au_{18}-Fibronectin Complexes with Time

To see if Au_{18}-fibronectin could be organized into fibrils after binding and if fibril formation occurred on the cell surface, subconfluent cultures of fibroblasts that contained little pre-existing matrix were incubated with Au_{18}-fibronectin for 1.5–5 h. These longer incubations resulted in the Au_{18}-fibronectin on the cell surface being arranged into linear arrangements or networks of extracellular fibrils. The fibrillar arrangements varied in length and density from cell to cell and from culture to culture. The areas ranged from 0.04 to 90×10^{-1} μm². The average area of a fibrillar arrangement was 12.5×10^{-1} μm². 16% of the fibroblasts contained only fibril-like arrangements of Au_{18}-fibronectin, 63% of the fibroblasts contained clusters of Au_{18}-fibronectin as well as fibril-like arrangements of the Au_{18}-fibronectin, and only 11% had clusters exclusively (Table I). In comparison, in cultures incubated with Au_{18}-fibronectin for 15–30 min, 63% of the fibroblasts contained only clusters of Au_{18}-fibronectin. In fibroblasts incubated with Au_{18}-fibronectin for 1.5–5 h, the fibrillar arrangements represented up to 11.3% of the area observed (Table II). The clusters of Au_{18}-fibronectin represented ~0.2% of the area observed. This is a two- to three-fold increase in the area occupied by the fibrillar arrangements of Au_{18}-fibronectin in the cells incubated for the longer times. The area represented by clusters of Au_{18}-fibronectin remained relatively unchanged with time.

Fig. 4 *A* shows Au_{18}-fibronectin arranged in a fibrillar network on the upper surface of an S132 fibroblast incubated with Au_{18}-fibronectin for 1.5 h. Much of the network, although not all of it, co-aligns with intracellular microfilament bundles (large arrows). The fibrillar networks of Au_{18}-fibronectin (small arrow) are frequently connected to filapods. These networks are also frequently observed to be connected to retraction fibers (data not shown). The filopodia appeared to pull the networks of Au_{18}-fibronectin off the cell surface and into the extracellular space. Au_{18}-fibronectin complexes underneath the cell are arranged in clusters, and fibrillar arrangements and networks of Au_{18}-fibronectin on the lower surface of the fibroblast are not observed.

Fig. 4 *B* shows a fibroblast (Detroit 551) incubated with Au_{18}-fibronectin for 3 h. The Au_{18}-fibronectin is found in large linear clusters arranged over bundles of intracellular microfilaments (large arrow). There do not appear to be fibrils connecting the Au_{18}-fibronectin in these clusters as there are along the edge of the cell (small arrows) and on the

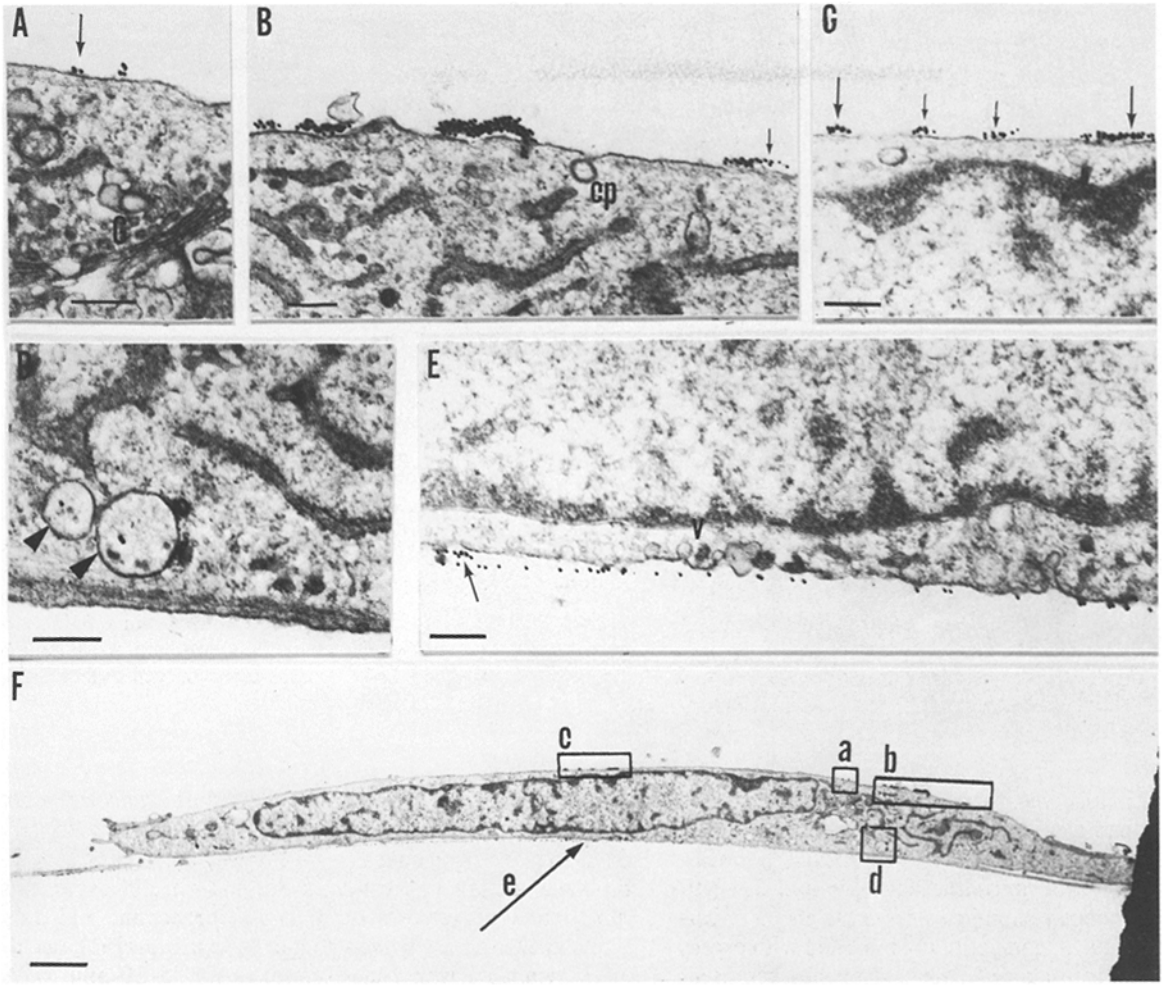

Figure 3. Conventional transmission electron micrograph of an A1-F human skin fibroblast incubated with Au_{18}-fibronectin for 30 min at 37°C. (*A*) Clusters of Au_{18}-fibronectin bound to the cell surface (*large arrow*). G, Golgi complex. (*B*) Clusters of Au_{18}-fibronectin bound to filamentous material on the dorsal cell surface (*small arrow*). CP, coated pit. (*C*) Cluster of Au_{18}-fibronectin bound to the cell surface (*large arrows*) and to filamentous material on the dorsal cell surface (*small arrows*). (*D*) Au_{18}-fibronectin complexes endocytosized by the cell (*arrowheads*). (*E*) Au_{18}-fibronectin complexes bound to filamentous material on the ventral surface of the fibroblast (*arrow*). Numerous vesicles are observed on the ventral surface (*V*). Au_{18}-fibronectin complexes are also observed bound to the substrate. (*F*) Longitudinal section of fibroblast shown in Figs. *A–E*. Bars: (*A–E*) 0.25 μm; (*F*) 1.0 μm.

cell in Fig. 4 *A*. These findings suggest that these linear, fibril-like arrangements may be bound to the cell surface. The appearance of these linear arrangements with time and the disappearance of small clusters of Au_{18}-fibronectin on top of the cell suggest that the Au_{18}-fibronectin is rearranged at specific regions of the upper surface of the fibroblast. That is, the linear arrangements observed in Fig. 4, *A* and *B* may represent intermediate stages of fibril formation, in which

Table II. Areas of the Cell Surface Containing Au_{18}-Fibronectin Clusters and Fibrils

Labeling conditions	Classification of cell according to distribution of label	Area			Area (percent of total)	
		Clusters	Fibrils	Total	Clusters	Fibrils
		μm^2	μm^2	μm^2		
Au_{18}-fibronectin (15–30 min)						
	Clusters	0.03	–	18.5	0.18	–
	Clusters and fibrils	0.03	0.41	20.1	0.14	2.0
	Fibrils	–	0.36	7.3	–	5.0
Au_{18}-fibronectin (1.5–5 h)						
	Clusters	0.03	–	10.7	0.24	–
	Clusters and fibrils	0.03	1.26	15.9	0.20	7.9
	Fibrils	–	0.56	5.0	–	11.3

The cells analyzed in Table I were further analyzed as described in Materials and Methods. The total area is a minimum inasmuch as the calculations did not take into account the ventral surface of the cell nor the curvature of the cell sides.

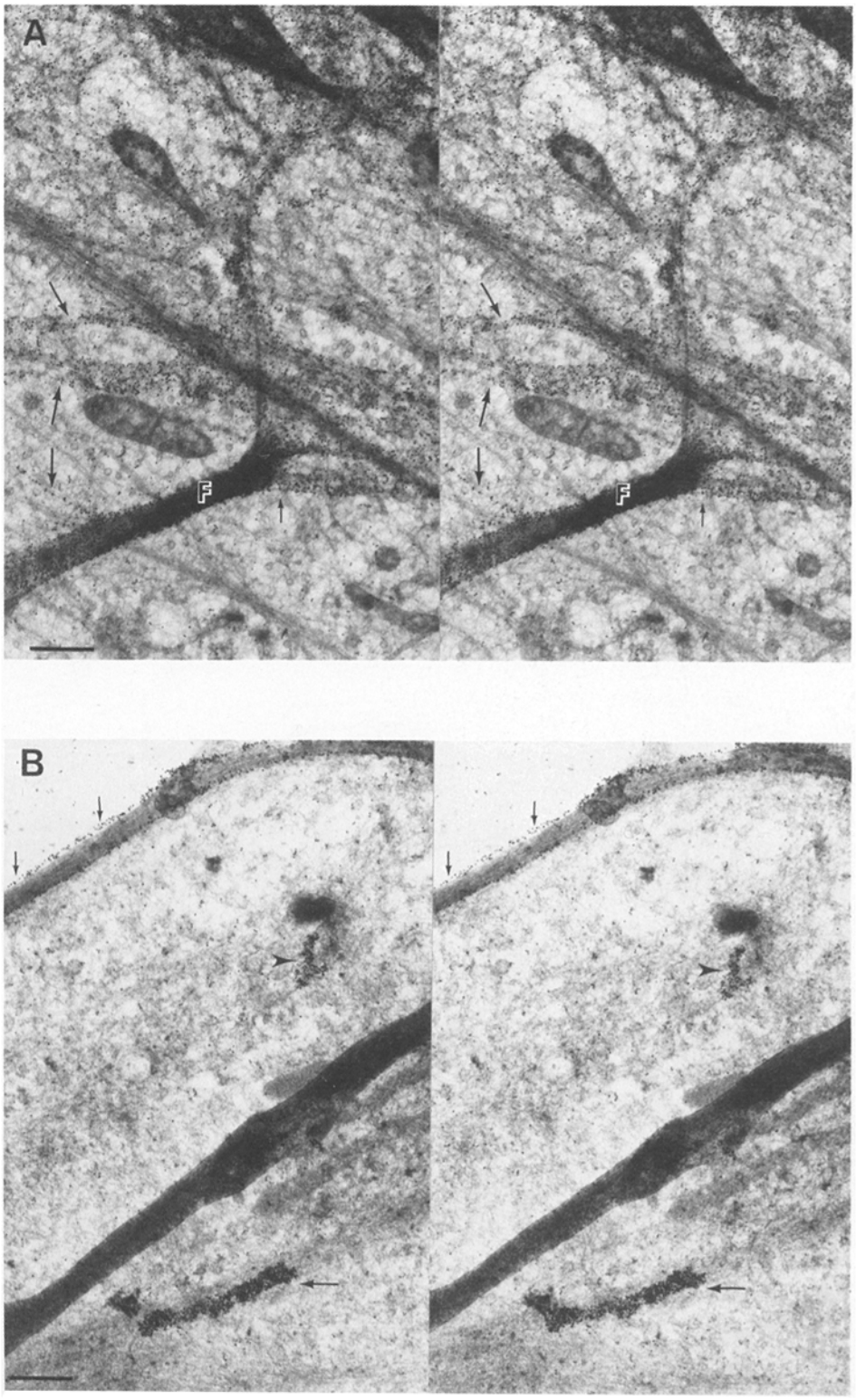

Figure 4. (*A*) A stereo micrograph of an S132 human skin fibroblast incubated with Au_{18}-fibronectin for 1.5 h at 37°C. A linear arrangement of Au_{18}-fibronectin is observed above intracellular bundles of microfilaments (*large arrows*). Au_{18}-fibronectin is also observed in networks of filaments on the dorsal surface of the cell (*small arrow*). Filaments of Au_{18}-fibronectin are frequently observed connected to filopodias (*F*). Stereo tilt 7° from horizontal. (*B*) A stereo micrograph of an S132 skin fibroblast incubated with Au_{18}-fibronectin for 3 h at 37°C. The fibroblast shows several different patterns of Au_{18}-fibronectin complexes bound to the cell surface. Arrowhead shows a cluster of Au_{18}-fibronectin on the ventral surface of the cell co-aligning with intracellular microfilaments. The large arrow shows a more linear arrangement of the Au_{18}-fibronectin complexes on the fibroblast dorsal surface. This cluster also appears to co-align with intracellular microfilament bundles. Small arrows show filaments containing Au_{18}-fibronectin attached to the edge of the cell. Stereo tilt 8° from horizontal. Bars, 0.5 μm.

fibronectin molecules are being brought together, disulfide-bonded, and translocated into the extracellular space.

Cell Surface Binding of Au_{18}-70-kD Fragment and Au_5-160–180-kD Fragments

To distinguish binding sites on the cell surface that are involved in matrix formation from other binding sites on fibronectin, fibroblasts were incubated with the 70-kD fragment that contains the amino-terminal gelatin- and heparin-binding sites located in the type I and II homology sequences and the 160–180-kD fragments that are lacking the amino and carboxyl type I homology sequences. The 160–180-kD fragment contains a second heparin-binding site (Sekiguchi et al., 1985) and the region of fibronectin that binds to a 140-kD

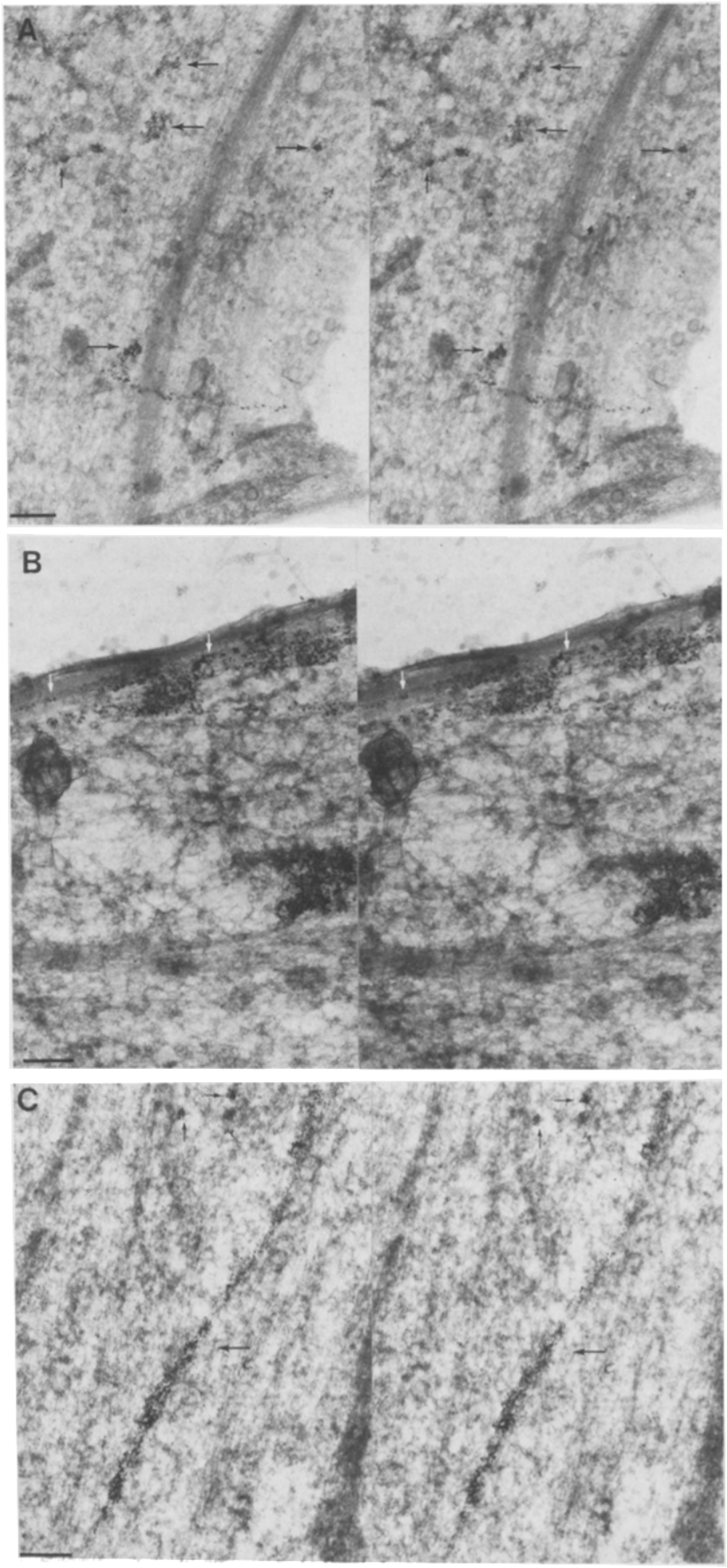

Figure 5. (*A*) A stereo micrograph of an A1-F human skin fibroblast incubated with Au_{18}-70-kD fragments for 30 min at 37°C. Clusters of Au_{18}-70-kD fragments on the dorsal surface of the cell co-align with intracellular bundles of microfilaments (*large arrows*). Small arrow shows Au_{18}-70-kD fragments in extracellular matrix fibrils. Stereo tilt 7° from horizontal. (*B*) A stereo micrograph of an A1-F skin fibroblast incubated with Au_{18}-70-kD fragments for 30 min. Linear arrangements of Au_{18}-70-kD fragments that co-align with intracellular microfilaments are observed along the edge of the cell (*arrows*). Stereo tilt 7° from horizontal. (*C*) A stereo micrograph of an A1-F skin fibroblast. A linear arrangement of Au_{18}-70-kD fragments is observed when A1-F skin fibroblasts are incubated with Au_{18}-70-kD fragments for 5 h at 37°C (*large arrow*). Small arrows show clusters of Au_{18}-70-kD fragments. Stereo tilt 8° from horizontal. (*D*) A whole mount of an A1-F human skin fibroblast incubated with Au_{18}-70-kD fragment complexes and a 100-fold excess of the 70-kD fragment for 30 min at 37°C. Arrows show scattered Au_{18}-70-kD fragments on the cell surface. Bars: (*A*) 0.25 μm; (*B–D*) 0.5 μm.

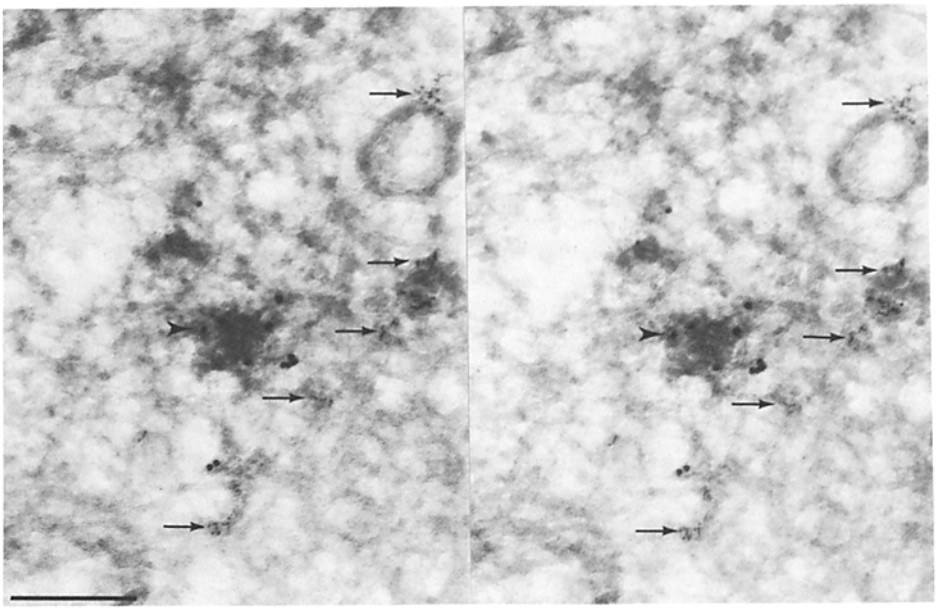

Figure 6. A stereo micrograph of an A1-F human skin fibroblast incubated with Au_{18}-70-kD fragments and Au_5-160–180-kD fragments for 30 min at 37°C. Arrows point to clusters of Au_5-160–180-kD fragments on the dorsal cell surface of the fibroblast. The arrowhead points to Au_{18}-70-kD fragments on the cell surface. The stereo micrograph is mounted so that the ventral surface of the fibroblast appears in the upper plane of the stereo micrograph. Stereo tilt 3° from horizontal. Bar, 0.25 μm.

cell surface receptor involved in cell adhesion and spreading (Pytela et al., 1985; Akiyama et al., 1986).

Fibroblasts labeled with Au_{18}-70-kD fragment showed a labeling pattern similar to that observed for cells labeled with Au_{18}-fibronectin. Fibroblasts (A1-F) incubated with Au_{18}-70-kD fragment for 30 min had clusters and some linear arrangements of complexes on the upper surface of the cell (Fig. 5, *A* and *B*). Some of the clusters and many of the linear arrangements co-aligned with intracellular microfilaments, as was the case with Au_{18}-fibronectin. A small percentage of the Au_{18}-70-kD complexes were arranged in clusters on the lower surface of the fibroblast. Linear arrangements of Au_{18}-70-kD fragment were not observed on the lower surface of the fibroblasts. Incubation of A1-F fibroblasts with Au_{18}-70-kD fragment for 5 h resulted in an increased number of linear, fibril-like arrangements and fewer clusters of the Au_{18}-70-kD fragment (Fig. 5 *C*). Some of the areas along these linear arrangements appear to coalign with intracellular microfilaments. The binding of Au_{18}-70-kD fragment was specific and could be blocked by incubating fibroblasts with excess 70-kD fragment. Fig. 5 *D* shows the cell surface of a fibroblast labeled with excess 70-kD fragment and Au_{18}-70-kD fragment for 30 min at 37°C. Clusters of Au_{18}-70-kD fragment and Au_{18}-70-kD fragment in linear arrangements are not present.

When A1-F fibroblast cultures were incubated with both Au_{18}-70-kD fragment and Au_5-160–180-kD fragments, the two gold complexes did not colocalize on the cell surface (Fig. 6). Binding of Au_5-160–180-kD fragments to cells was sparse. Many of the Au_5-160–180-kD fragments bound in small clusters predominantly on the lower surface of the cell near the ruffling edge of the fibroblast. Linear arrangements and fibrillar networks of the Au_5-160–180-kD fragments were not observed. In some cells however, discrete patches of Au_5-160–180-kD fragments were distributed along a diagonal line.

Discussion

The incorporation of fibronectin into the extracellular matrix of cultured human skin fibroblasts reportedly is a receptor-mediated process (McKeown-Longo and Mosher, 1983, 1984, and 1985). These previous studies showed that exogenously added I^{125}-plasma fibronectin binds to the cell layer of cultured human fibroblasts in two distinguishable pools. In pool I, binding of fibronectin is reversible, and bound fibronectin is soluble in deoxycholate. Pretreatment of cells with low concentrations of trypsin to remove pre-existing matrix has no effect on pool I binding, and pretreatment of cells with cycloheximide to block synthesis of endogenous fibronectin does not decrease pool I binding (McKeown-Longo and Mosher, 1985). More recently, Allen-Hoffmann and Mosher (1985 and unpublished observations) have shown that pool I binding can be down-regulated with cholera toxin or up-regulated with transforming growth factor beta within 30 min after exposure to the agent. Such a rapid effect is more consistent with labile binding sites on the cell surface than with static binding sites in pre-existing matrix.

The properties of fibronectin in pool I, together with fluorescence microscopic studies (McKeown-Longo and Mosher, 1983; 1985), suggest that fibronectin in pool I is binding to a cell surface receptor rather than matrix fibrils. It should be noted that studies by Chernousov et al. (1985) suggest that intact fibronectin and the 70-kD amino-terminal fragment bind to pre-existing matrix. However, the shortest incubation time used in these studies was 3 h and the concentration of the ligands used was 500 μg/ml (7×10^{-6} M for the 70-kD fragment and 10^{-6} M for intact fibronectin). These concentrations are much higher than the K_d for the binding to the matrix assembly receptor (3×10^{-8} M). When McKeown-Longo and Mosher (1983) attempted to saturate pool I binding, there was a considerable nonsaturable component, so that for fibronectin concentrations >35 μg/ml (7×10^{-8} M), more than 50% of total binding was nonsaturable. We noted that binding of Au_{18}-fibronectin to pre-existing matrix was not blocked by excess unlabeled fibronectin. Thus, we suspect that most of the binding noted by Chernousov et al. (1985) was to lower affinity or nonsaturable sites in the extracellular matrix, e.g., to collagen, glycosaminoglycan, or already assembled fibronectin fibrils.

In the present studies we examined whole mounts of subconfluent cultures of fibroblasts by HVEM to localize fibronectin in pool I for possible cell surface interactions involved in the assembly of fibronectin fibrils. Subconfluent cultures were primarily studied rather than confluent cultures because the subconfluent cultures actively produced an extracellular fibronectin matrix. We found that Au_{18}-fibronectin initially bound to the cell surface in clusters above bundles of microfilaments. These clusters were primarily located along the edge of the fibroblast. The clustering pattern of Au_{18}-fibronectin found in these micrographs is reminiscent of the short striae of fibronectin observed in immunofluorescence studies of young cultures of NIL8 cells (Hynes and Destree, 1978). In the NIL8 cells, the observed striae coaligned with actin bundles by double antibody immunofluorescence. Such tiny fibrils and patches were also observed by fluorescence microscopy of confluent fibroblast cultures labeled with FITC-fibronectin for 20 min (McKeown-Longo and Mosher, 1983). These fibrils and patches of FITC-fibronectin were thought to represent soluble fibronectin bound to the cell layer but not disulfide cross-linked into insoluble matrix fibrils.

Conventional transmission electron microscopy showed that specifically bound Au_{18}-fibronectin was not associated with filamentous cell surface matrix components but attached to the cell surface. Therefore, Au_{18}-fibronectin is initially not bound to cell surface collagen, despite the fact that fibronectin has been shown to co-distribute with procollagen in the pericellular matrix (Bornstein and Ash, 1977; Vaheri et al., 1978). To establish this point further, we have done fluorescence microscopy and HVEM on cultures pretreated with collagenase and then incubated with exogenous FITC–fibronectin or Au_{18}-fibronectin and found patterns of binding similar to those of untreated cells (unpublished observations).

Some of the Au_{18}-fibronectin binding after 15–30 min was found in fibrillar structures on the cell surface or in extracellular matrix in ~15% of the fibroblasts. Fibrillar Au_{18}-fibronectin was much more extensive after longer incubations. Fibrillar membrane-associated material was patchy in appearance and ~19 nm from the cell surface in transmission electron micrographs. Hedman et al. (1978) observed that in young cultures ferritin–antifibronectin complexes localized 25 nm or less from the cell surface. This Au_{18}-fibronectin may therefore represent membrane-associated fibronectin that has started to be assembled into matrix fibrils.

Insoluble rod-like fibronectin complexes can be formed in the absence of cells if the fibronectin is precipitated with heparin (Jilek and Hörmann, 1979) or polyamines (Vuento et al., 1980). However, ultrastructural studies on fibronectin fibril formation in vitro using collagen gels, heparin, hyaluronic acid, chondroitin sulfate, or chondroitin sulfate proteoglycan have not recapitulated the assembly of fibronectin fibrils in vivo (Turley et al., 1985). In addition, we observed that fibronectin fibrils were not formed under culture conditions similar to those used in this study unless cells were present. Thus, it seems reasonable to conclude that a preassembled matrix alone is not sufficient to assemble fibronectin fibrils and that some aspects of fibronectin fibril assembly are controlled by cells.

Au_{18}-fibronectin was bound to cells over a 5-h period to visualize possible cell surface events involved in the assembly of fibronectin fibrils (pool II). With longer incubations, Au_{18}-fibronectin on the upper surface of the fibroblast became arranged into linear arrangements as well as into fibrillar networks. A linear rearrangement of Au_{18}-fibronectin on the cell surface was also observed when the cultures were incubated with Au_{18}-fibronectin for 15 min, washed, and incubated for an additional hour without conjugate (unpublished observation). The linear arrangements were frequently found near retracting fibers and filopods. The arrangements may represent intermediate stages of fibrillogenesis. Fibronectin fibrillogenesis may therefore occur when the fibronectin molecules bound to the matrix assembly receptor on the cell surface are brought into contact with other fibronectin-receptor complexes on the cell surface. The intracellular microfilaments observed underneath the cell surface fibronectin may be responsible for bringing together and aligning the fibronectin molecules in such a way that disulfide exchange can occur to form a fibril.

This rearrangement of fibronectin into fibrillar structures on the cell surface appears to involve interactions between the fibroblast cell surface and the 70-kD amino terminal type I and II homology units of fibronectin (McKeown-Longo and Mosher, 1985). Cultures double-labeled with the amino-terminal 70-kD fragment and the 160–180-kD fragments (which lack Type I and II homology units), showed that the amino-terminal 70-kD fragment and the 160–180-kD fragments did not colocalize. Because the 160–180-kD fragments contain the cell adhesion site of fibronectin and a strong heparin-binding site, the matrix assembly sites for fibronectin on cells must be distinct from the RDGS and heparin binding sites. Incubation of the Au_{18}-70-kD fragment for longer periods of time resulted in the rearrangement of Au_{18}-70-kD fragments into linear patterns along the edge of the fibroblast. These linear arrangements may represent the intermediate fibril-like arrangements discussed above, since the 70-kD fragment does not form disulfide multimers and does not enter the extracellular matrix (McKeown-Longo and Mosher, 1985).

Our finding that little of the 160–180-kD fragments bound to cells is consistent with the findings of Chernousov et al. (1985), who noted that two FITC–60-kD fragments of fibronectin that contained the cell adhesion site of fibronectin and a heparin-binding site bound poorly to cell layers. Many of the cell adhesion sites presumably are occupied with preexisting fibronectin. Monoclonal antibodies against the cell adhesion receptor showed that the cell adhesion receptor was localized to areas surrounding the termini of actin in stress fibers (Damsky et al., 1985) and colocalized with vinculin and α-actinin at extracellular matrix contacts (Duband et al., 1986; Chen et al., 1985). The 140-kD cell adhesion receptor was not localized within focal contacts at the cell periphery or on the upper (dorsal) surface of cells (Chen et al., 1985), nor did it colocalize with bundles of actin along the lateral edges of the cell (Duband et al., 1986).

However, the regions along the lateral edges of the fibroblast where fibronectin fibrillogenesis appears to take place and Au_{18}-70-kD fragment binds are rich in intracellular microfilament bundles that appear to be actin filaments based on their size and location. The close association among Au_{18}-fibronectin or Au_{18}-70-kD complexes and microfilament filaments along the lateral edges of the cell and the absence of Au_5-160–180-kD fragments in these regions suggest

that there are two modes of fibronectin–microfilament interactions, one mediated by the cell adhesion receptor and one mediated by the matrix assembly receptor. The existence of two fibronectin–microfilament interactions raises the question as to whether the fibronexus described by Singer (1979) may represent regions on the cell surface other than sites of cell adhesion where fibronectin fibrillogenesis is occurring. Further studies using culture conditions identical to those used by Singer would be needed to answer this question.

The authors wish to express their appreciation for the technical assistance and advice of Drs. Hans Ris, Ralph Albrecht, Joseph Loftus, and James Pawley.

This study was supported by grant HL-21644 from the National Institutes of Health and by a grant from the American Heart Association, Wisconsin Affiliate.

Received for publication 8 March 1986, and in revised form 22 September 1986.

References

Allen-Hoffmann, B. L., and D. F. Mosher. 1985. Fibronectin matrix assembly receptor number is decreased in normal human fibroblasts after treatment with cholera toxin. *J. Cell Biol.* 101(5, Pt. 2):9a. (Abstr.)

Akiyama, S. K., S. S. Yamada, and K. M. Yamada. 1986. Characterization of a 140-kD avian cell surface antigen as a fibronectin-binding molecule. *J. Cell Biol.* 102:442–448.

Balian, G. E., E. M. Click, E. Crouch, J. M. Davidson, and P. Bornstein. 1979. Isolation of a collagen-binding fragment from fibronectin and cold-insoluble globulin. *J. Biol. Chem.* 254:1429–1432.

Bornstein, P., and J. F. Ash. 1977. Cell surface-associated structural proteins in connective tissue cells. *Proc. Natl. Acad. Sci. USA.* 74:2480–2484.

Chen, W. T., E. Hasegawa, T. Hasegawa, C. Weinstock, and K. M. Yamada. 1985. Development of cell surface linkage complexes in cultured fibroblasts. *J. Cell Biol.* 100:1103–1114.

Chernousov, M. A., M. L. Metsis, and V. E. Koteliansky. 1985. Studies of extracellular fibronectin matrix formation with fluoresceinated fibronectin and fibronectin fragments. *FEBS (Fed. Eur. Biochem. Soc.) Lett.* 183:365–369.

Damsky, C. H., K. A. Knudsen, D. Bradley, C. A. Buck, and A. F. Horwitz. 1985. Distribution of the cell substratum attachment (CSAT) antigen on myogenic and fibroblastic cells in culture. *J. Cell Biol.* 100:1528–1539.

Duband, J.-L., S. Rocher, W.-T. Chen, K. M. Yamada, and J. P. Thiery. 1986. Cell adhesion and migration in the early vertebrate embryo: location and possible role of the putative fibronectin receptor complex receptor complex. *J. Cell Biol.* 102:160–178.

Engvall, E., and E. Ruoslahti. 1977. Binding of soluble form of fibroblast surface protein, fibronectin to collagen. *Int. J. Cancer.* 20:1–5.

Geoghegan, W. D., and A. Ackerman. 1977. Absorption of horseradish peroxidase, ovomucid, and anti-immunoglobulin to colloidal gold for the indirect detection of concanvalin A, wheat germ agglutinin and goat anti-human immunoglobulin G on cell surfaces at the electron microscopic level: a new method, theory and application. *J. Histochem. Cytochem.* 25:1187–1200.

Hayman, E. G., and E. Ruoslahti. 1979. Distribution of fetal bovine serum fibronectin and endogenous rat cell fibronectin in extracellular matrix. *J. Cell Biol.* 83:255–259.

Hedman, K., A. Vaheri, and J. Wartiovaara. 1978. External fibronectin of cultured human fibroblasts is predominantly a matrix protein. *J. Cell Biol.* 76:748–760.

Horisberger, M., and J. Rosset. 1977. Colloidal gold, a useful marker for transmission and scanning electron microscopy. *J. Histochem. Cytochem.* 25:295–305.

Hynes, R. O. 1985. Molecular biology of fibronectin. *Annu. Rev. Cell Biol.* 1:67–90.

Hynes, R. O., and A. T. Destree. 1978. Relationship between fibronectin (LETS protein) and actin. *Cell.* 15:875–886.

Jilek, F., and H. Hörmann. 1979. Fibronectin (cold insoluble globulin) VI. Influence of heparin and hyaluronic acid on the binding of native collagen. *Hoppe-Seyler's Z. Physiol. Chem.* 360:597–603.

Kornblihtt, A. R., K. Vibe-Pederson, and F. E. Baralle. 1984. Human fibronectin: molecular cloning evidence for two mRNAs species differing by an internal segment coding for a structural domain. *EMBO (Eur. Mol. Biol. Organ.) J.* 3:221–226.

Maupin, P., and T. D. Pollard. 1983. Improved preservation and staining of HeLa cell actin filaments, clathrin-coated membranes, and other cytoplasmic structures by tannic acid-glutaraldehyde-saponin fixation. *J. Cell Biol.* 96: 51–62.

McKeown-Longo, P. J., and D. F. Mosher. 1983. Binding of plasma fibronectin to cell layers of human skin fibroblasts. *J. Cell Biol.* 97:466–472.

McKeown-Longo, P. J., and D. F. Mosher. 1984. Mechanisms of formation of disulfide-bonded multimers of plasma fibronectin in cell layers of cultured human fibroblasts. *J. Biol. Chem.* 259:12210–12215.

McKeown-Longo, P. J., and D. F. Mosher. 1985. Interactions of the 70,000-mol-wt amino-terminal fragment of fibronectin with the matrix-assembly receptor of fibroblasts. *J. Cell Biol.* 100:364–374.

Mosher, D. F. 1984. Physiology of fibronectin. *Annu. Rev. Med.* 35: 561–575.

Mosher, D. F., and R. B. Johnson. 1983. In vitro formation of disulfide-bonded fibronectin multimers. *J. Biol. Chem.* 258:6595–6601.

Oh, E., M. Pierschbacher, and E. Ruoslahti. 1981. Deposition of plasma fibronectin in tissues. *Proc. Natl. Acad. Sci. USA.* 78:3218–3221.

Pierschbacher, M. D., E. G. Hayman, and E. Ruoslahti. 1981. Location of the cell attachment site in fibronectin with monoclonal antibodies and proteolytic fragments of the molecule. *Cell.* 26:259–267.

Pytela, R., M. D. Pierschbacher, and E. Ruoslahti. 1985. Identification and isolation of a 140 kd cell surface glycoprotein with properties expected of a fibronectin receptor. *Cell.* 40:191–198.

Ris, H. 1985. The cytoplasmic filament system in critical point-dried whole mounts and plastic-embedded sections. *J. Cell Biol.* 100:1474–1487.

Schwarzbauer, J. E., J. I. Paul, and R. O. Hynes. 1985. On the origin of species of fibronectin. *Proc. Natl. Acad. Sci. USA.* 82:1424–1428.

Sekiguchi, K., A. Siri, L. Zardi, and S.-I. Hakomori. 1985. Differences in domain structure between human fibronectins isolated from plasma and from culture supernatants of normal and transformed fibroblasts. *J. Biol. Chem.* 260:5105–5114.

Singer, I. I. 1979. The fibronexus: a transmembrane association of fibronectin-containing fibers and bundles of 5 nm microfilaments in hamster and human fibroblasts. *Cell.* 16:675–685.

Tamkun, J. W., and R. O. Hynes. 1983. Plasma fibronectin is synthesized and secreted by hepatocytes. *J. Biol. Chem.* 245:5728–5736.

Trelstad, R. L., and K. Hayashi. 1979. Tendon fibrillogenesis: intracellular collagen subassemblies and cell surface changes associated with fibril growth. *Dev. Biol.* 71:228–242.

Turley, E. A., C. A. Erickson, and R. P. Tucker. 1985. The retention and ultrastructural appearances of various extracellular matrix molecules incorporated into three-dimensional hydrated collagen lattices. *Dev. Biol.* 109: 347–369.

Vaheri, A., M. Kurkinen, V.-P. Lehto, E. Linder, and R. Timpl. 1978. Codistribution of pericellular matrix proteins in cultured fibroblasts and loss in transformation: fibronectin and procollagen. *Proc. Natl. Acad. Sci. USA.* 75:4944–4948.

Vuento, M., T. Vartio, M. Saraste, C. H. von Bondsorff, and A. Vaheri. 1980. Spontaneous and polyamine-induced formation of filamentous polymers from soluble fibronectin. *Eur. J. Biochem.* 105:33–42.

Williams, E. C., P. A. Janmey, R. B. Johnson, and D. F. Mosher. 1983. Fibronectin: effect of disulfide bond reduction on its physical and functional properties. *J. Biol. Chem.* 258:5911–5914.

Wolosewick, J. J., and K. R. Porter. 1976. Stereo high voltage electron microscopy of whole cells of the human diploid line, WI-38. *Am. J. Anat.* 147:303–324.